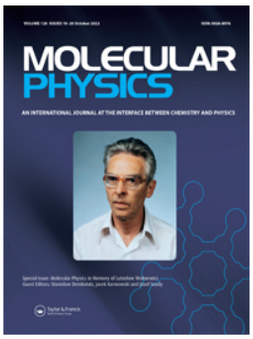

Taylor & Francis
Taylor & Francis Group

Molecular Physics

An International Journal at the Interface Between Chemistry and Physics

ISSN: (Print) (Online) Journal homepage: https://www.tandfonline.com/loi/tmph20

Electron affinity of LiH^-

Saeed Nasiri, Ludwik Adamowicz & Sergiy Bubin

To cite this article: Saeed Nasiri, Ludwik Adamowicz & Sergiy Bubin (2022) Electron affinity of LiH^-, Molecular Physics, 120:19-20, e2065375, DOI: 10.1080/00268976.2022.2065375

To link to this article: https://doi.org/10.1080/00268976.2022.2065375

Published online: 21 Apr 2022.

MOLECULAR PHYSICS
2022, VOL. 120, NOS. 19–20, e2065375 (8 pages)
https://doi.org/10.1080/00268976.2022.2065375

Taylor & Francis
Taylor & Francis Group

L. WOLNIEWICZ SPECIAL ISSUE

Electron affinity of LiH^-

Saeed Nasiri[a], Ludwik Adamowicz[b,c,d] and Sergiy Bubin[a]

[a]Department of Physics, Nazarbayev University, Nur-Sultan, Kazakhstan; [b]Department of Chemistry and Biochemistry, University of Arizona, Tucson, AZ, USA; [c]Department of Physics, University of Arizona, Tucson, AZ, USA; [d]Centre for Advanced Study (CAS), the Norwegian Academy of Science and Letters, Oslo, Norway

ABSTRACT

In this work we present high-accuracy benchmark-quality calculations of the electron affinity (EA) of the LiH molecule in a framework that does not assume the Born–Oppenheimer (BO) approximation. The EA is calculated as a difference between the total energies of LiH^- and LiH. The calculations of the energies are performed using the Rayleigh-Ritz variational method with large basis sets of all-particle explicitly correlated Gaussian functions (ECGs). Up to 14,000 ECGs are used in the calculations for each system. The nonlinear parameters of the ECGs are optimised by by the minimisation of the total non-relativistic energy of the system using an approach that employs the energy gradient determined with respect the parameters. The LiH^- and LiH non-relativistic non-BO wave functions are subsequently used to calculate the leading relativistic corrections. The calculated EA is well converged in terms of the size of the basis sets and the obtained value falls within the uncertainty of the best available experimental result.

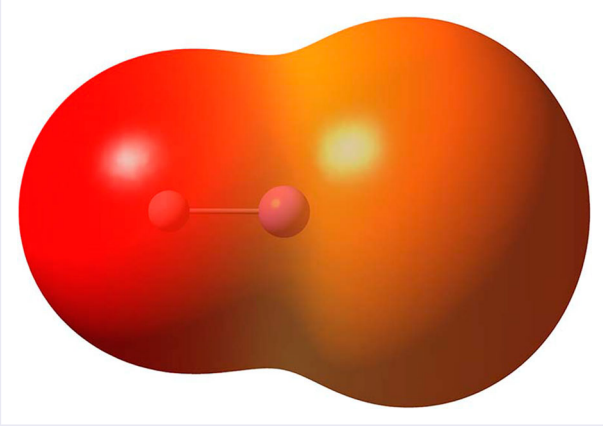

ARTICLE HISTORY
Received 11 February 2022
Accepted 7 April 2022

KEYWORDS
Electron affinity; explicitly correlated basis sets; non-Born–Oppenheimer

1. Introduction

Since its emergence about a century ago, the main task of quantum chemistry has been the development of methods for performing high accuracy calculations of molecules based of the first principles of quantum mechanics. Widespread adoption of electronic computers in scientific research in 1960s brought the capability of predicting the spectra of atoms and molecules at the quantum-mechanical level of theory to new heights. One of the most spectacular successes of computational quantum chemistry at the time has been a series of works by Kołos and Wolniewicz regarding the hydrogen molecule [1–3].

Regardless of their specifics, first principles calculations have to involve a certain number of approximations. One of the most important and commonly used one in the molecular structure theory is the Born–Oppenheimer approximation, which makes an assumption that the electronic and nuclear motions in molecules can be separated. While it works quite well (even quantitatively) in most chemical systems, there are some uncertainties that are associated with it. Indeed, in

CONTACT Sergiy Bubin sergiy.bubin@nu.edu.kz Department of Physics, Nazarbayev University, Nur-Sultan010000, Kazakhstan

their early works Kołos and Wolniewicz already recognised that some discrepancy between the binding energy of H_2 they had calculated was likely be due to the adiabatic approximation involved [2].

As the number-crunching power of computers keeps growing over the years, it becomes possible, at least for the smallest molecular systems, to reduce the number of approximations to a minimum. In the approach adopted in this work we consider few-electron diatomic systems, LiH and LiH^-, without the use of the Born–Oppenheimer approximation. This means that all particles, i.e. the nuclei and electrons forming the molecule, are treated on an equal footing. Such an approach, if it only concerns the internal bound states of the system, necessitates that the centre of mass motions is removed from the Hamiltonian. This separation in the non-BO method we have developed is done by starting with the total non-relativistic Hamiltonian of the molecule written in terms of laboratory Cartesian coordinates and then transforming it to a new Cartesian coordinate system. The first three coordinates in this new system are the centre-of-mass laboratory Cartesian coordinates and the remaining $3N-3$ coordinates, where N is the sum of the number of the nuclei and the number of the electrons in the molecule, are internal coordinates. In our approach, the internal coordinates $\mathbf{r}_{i-1} = \mathbf{R}_i - \mathbf{R}_1$ are the Cartesian coordinates of vectors with the origins at a chosen reference particle located at $\mathbf{R}_1$ (usually the heaviest nucleus in the system, which we can call particle 1) and ending at the positions of particles $2, 3, \ldots, N$. A transformation of the total non-relativistic Hamiltonian to the new coordinates system results in its rigorous separation of the lab-frame Hamiltonian into an operator that represents the kinetic energy of the centre-of-mass motion and an internal Hamiltonian, as described in the next section. The centre-of-mass kinetic energy Hamiltonian depends only on the centre-of-mass laboratory coordinates and the internal Hamiltonian depends only on the internal coordinates [4].

The second approximation, as will be demonstrated in the results section in this work, we effectively reduce to a negligible impact is the incompleteness of the basis set used to expand the total non-BO non-relativistic wave function of the system. In our approach this is done by using a large number of all-particle explicitly correlated Gaussian functions (ECGs) for expanding the system's wave function and by performing a thorough variational optimisation of the nonlinear parameters of the Gaussians. We employ a procedure that involves the use of the analytical gradient of the total energy of the system determined with respect these parameters. The explicit dependence of the Gaussian of the inter-particle distances is key in achieving high accuracy in the calculations. Even though the correlated Gaussian do not strictly fulfill the Kato conditions for the behaviour of the wave function at the inter-particle coalescent points, and their amplitude drops too rapidly when the distances approach infinity, if a large number of ECGs is used in the calculation, these deficiencies can be effectively remedied, as shown in this work.

The third approximation, whose impact on the results needs to be reduced is the neglect of higher-order relativistic and quantum electrodynamics effects. In the present work we only consider the former. The calculations of the leading relativistic corrections are done in the framework of the first-order perturbation theory. The corrections are calculated as the expectation values of the operators representing the corrections using the non-BO non-relativistic wave function.

In our previous work published almost 18 years ago [5] we presented non-BO calculations of LiH, LiH^-, LiD, and LiD^- performed with a much smaller basis of 3600 ECGs. The relativistic effects were not included in those calculations at all. In the present work, the size of the basis sets used in the calculations are increased nearly four-fold. This, as well as the inclusion of leading relativistic corrections, allows for a significant increase of the accuracy of the results.

LiH^- is the smallest stable diatomic anion of a stable molecule. Its adiabatic electron detachment (ED) energy has been investigated both experimentally [6–9] and theoretically [10–14]. These include our previous work [5].

The LiH/LiH^- system is small enough to be studied at the highest level of the theoretical sophistication [10–14]. Thus, it is a good model for assessing the accuracy and performance of the various computational approaches including the present approach. Also, theoretical calculations can be compared with experimental measurements of the LiH electron affinity [6–9] of which the value of 0.342 ± 0.012 eV reported by Sarkas *et al.* [9] is currently the most accurate one. This value, as well as the corresponding value of the electron affinity of the LiD molecule, was reproduced within the experimental error bars in our previous calculations performed without including the relativistic corrections. In the present calculations we increase the level of theory by the addition of the relativistic corrections and reducing the basis runcation uncertainty by means of increasing the size of the basis set. The calculated LiH electron affinity obtained in the present work, to the best of our knowledge, is the most precise value obtained in direct calculations based of the first principles. We hope that this work will motivate new measurements of the LiH electron affinity at a much higher level of accuracy.

Table 1. Variational non-Born–Oppenheimer non-relativistic energies (E_{nr}) of the ground states of of LiH and LiH^- molecules and the corresponding total relativistic energies (E_{rel}) obtained by adding the MV, OO, D, and SS relativistic corrections (also shown in the table) to the E_{nr} energies.

	Basis	E_{nr}	$\langle H_{MV}\rangle$	$\langle H_{OO}\rangle$	$\langle H_{D}\rangle$	$\langle H_{SS}\rangle$	E_{rel}
LiH	8,000	−8.06643754	-79.0353	-0.473082	63.9136	3.4608	−8.06708369
	10,000	−8.06643877	−79.0459	−0.473069	63.9249	3.4579	−8.06708504
	12,000	−8.06643887	−79.0534	−0.473065	63.9332	3.4552	−8.06708525
	14,000	−8.06643898	−79.0542	−0.473066	63.9341	3.4550	−8.06708535
	∞	−8.06643910(6)					−8.06708553(9)
LiH^-	8,000	−8.07866211	−78.8561	−0.471358	63.7704	3.4497	−8.07930685
	10,000	−8.07866960	−78.8697	−0.471362	63.7845	3.4494	−8.07931433
	12,000	−8.07867342	−78.9278	−0.471361	63.8394	3.4488	−8.07931834
	14,000	−8.07867612	−78.9306	−0.471360	63.8436	3.4470	−8.07932107
	∞	−8.0786771(5)					−8.0793223(6)

Notes: Results obtained with basis sets of different size are shown. Note that the generation of the largest set of 14,000 ECGs involved somewhat more extensive optimisation. The values in parentheses are uncertainties due to the finiteness of basis set used. All energies and expectation values are expressed in atomic units.

2. Method

When accurate wave functions corresponding to the solution of the non-relativistic problem are available, the most practical approach to account for small in magnitude relativistic and QED effects in light atoms is to use the perturbation theory. In this approach, the total energy can be expanded in powers of the fine structure constant, α [15,16]:

$$E_{\rm tot} = E_{\rm nr} + \alpha^2 E^{(2)}_{\rm rel} + \alpha^3 E^{(3)}_{\rm QED} + \cdots, \qquad (1)$$

where E_{nr} is the non-relativistic energy of the state being considered, the second term ($\alpha^2 E^{(2)}_{rel}$) represents the leading relativistic corrections, the third term ($\alpha^3 E^{(3)}_{QED}$) represents the leading QED corrections, and so on. Each of these terms is evaluated as an expectation value of a certain effective operator.

As mentioned, the non-relativistic calculations in the present work are carried out using a Hamiltonian that represents the internal state of the molecule and excludes the motion of the centre of mass, i.e. excludes the translational motion of the system as a whole. The internal Hamiltonian expressed in terms of the internal Cartesian coordinates, $\mathbf{r}_i$, $i = 1, \ldots, n$, where $n = N-1$ and N is the number of particles (electrons and nuclei) forming the molecule, as follows [4,17]:

$$\hat{\rm H} = -\frac{1}{2}\left(\sum_{i=1}^{n}\frac{1}{\mu_i}\nabla'_{\mathbf{r}_i}\nabla_{\mathbf{r}_i} + \frac{1}{m_0}\sum_{\substack{i,j=1\\ i\neq j}}^{n}\nabla'_{\mathbf{r}_i}\nabla_{\mathbf{r}_j}\right) + \sum_{i=1}^{n}\frac{q_0 q_i}{r_i} + \sum_{i>j=1}^{n}\frac{q_i q_j}{r_{ij}}, \qquad (2)$$

where m_0 is the mass of the reference nucleus (in the present calculations, the lithium nucleus) and q_0 is its charge, q_i are the charges of the other particles, $\mu_i = m_0 m_i/(m_0 + m_i)$ is the reduced mass of particle i (m_i, $i = 1, \ldots, n$, are the particle masses), r_i, $i = 1, \ldots, n$ is the distance from particle $i+1$ to the reference particle, i.e. particle 1, and r_{ij} is the distance between particle $j+1$ and particle $i+1$. The prime symbol in (2) denotes the matrix/vector transposition. One can notice that the internal Hamiltonian represents the motion of n particles, whose charges are the original particle charges, but the masses are the reduced masses (because of that, one can use the term 'pseudoparticles' to denote the particles described by the internal Hamiltonian (2)), in the central field of the charge of the reference nucleus. Thus, the internal Hamiltonian is invariant upon all rotations about the centre of the internal coordinate system and one can think of it as an 'atom-like' Hamiltonian. The eigenfunctions of this Hamiltonian can be classified using the same symmetries as the wave functions of atoms. In particular, the ground-state solution is spherically symmetric, i.e. it is invariant under rotations in 3D. This rotational symmetry takes place for the ground state of both LiH and LiH^-.

The approach used to obtain the internal Hamiltonian (2) and to separate out the centre-of-mass motion from the laboratory frame Hamiltonian is a generalisation of the standard textbook approach used to reduce a two-body problem to a one-body problem in quantum mechanics, e.g. in the case of an electron and proton forming the hydrogen atom. In the present work, the non-relativistic energies, E_{nr}, and the corresponding wave functions of LiH and LiH^- are calculated using this internal Hamiltonian.

The following all-particle spherically-symmetric explicitly correlated Gaussian functions are used in the present calculations:

$$\phi_k = r_1^{m_k}\exp[-\mathbf{r}'(A_k \otimes I_3)\mathbf{r}], \qquad (3)$$

where r_1 is the distance between the nuclei (particle 1 is the lithium nucleus while particle 2 is the proton), m_k is

an even integer from an extented range (in this work we adopted the range from 0–200) that can be viewed as an integer variational parameter, A_k is an $n \times n$ real symmetric matrix of the continuous exponential variational parameters, $\otimes$ denotes the Kronecker product, and I_3 is an 3×3 identity matrix. Note that both A_k and m_k are unique and independently tunable for each basis function, which is indicated by the presence of index k. Vector $\mathbf{r}$ in (3) is a $3n$-component vector formed by stacking the internal Cartesian coordinates $\mathbf{r}_i$:

$$\mathbf{r} = \begin{pmatrix} \mathbf{r}_1 \\ \mathbf{r}_2 \\ \vdots \\ \mathbf{r}_n \end{pmatrix} = \begin{pmatrix} x_1 \\ y_1 \\ z_1 \\ \vdots \\ x_n \\ y_n \\ z_n \end{pmatrix}. \tag{4}$$

Let us denote $A_k \otimes I_3$ as $\mathbf{A}_k$. This matrix $\mathbf{A}_k$ and, by extension, A_k, have to be positive definite is order for Gaussian (3) to be square integrable. To ensure positive definiteness of $\mathbf{A}_k$ we adopt the following Cholesky-factored form of it: $\mathbf{A}_k = (L_k L_k') \otimes I_3$, where L_k is a $n \times n$ lower-triangular matrix of real numbers. In this form, $\mathbf{A}_k$ is automatically positive definite for the L_k matrix elements being any real numbers. The L_k matrix elements are parameters that are variationally optimised in the present calculations. The optimisation employs the analytical energy gradient determined with respect to the L_k matrix elements. These elements can be varied without any restrictions in the range of values from $-\infty$ to $+\infty$. In addition to the optimisation of the L_k matrix elements, the m_k powers of r_1 that appear in (3) are also partially optimised.

The need to include the $r_1^{m_k}$ factor in Gaussian (3) can be explained by analysing the internal Hamiltonian (3). One notices that pseudoparticle 1 in the internal Hamiltonian (2) is a proton. Because of the strong Coulombic repulsion between this proton and the reference particle, located at the centre of the internal coordinate system, the density of pseudoparticle 1 must be virtually zero at this centre. At the same time for a diatomic molecule it sharply peaks at a sphere with the radius approximately equal to the equilibrium distance of the molecule. As an origin-centred Gaussian function has a maximum at the centre of the coordinate system, it needs to be modified to move its maximum away from the centre and to reach a maximum value on the mentioned sphere. This is accomplished by multiplying the Gaussians by the $r_1^{m_k}$ factors. Such factors, in addition to describing the shifting of the Gaussian maximum away from the coordinate system, are needed to describe the radial oscillations of the wave functions corresponding to excited states. If the Gaussians used in the calculation are spherically symmetric, as are basis functions (3), then all excited states they can describe are purely 'vibrational' states, i.e. states with the zero total angular momentum. Term 'vibrational' is put is quotes because in a non-BO calculations vibrational and electronic motions couple and strictly speaking the vibrational quantum number is not a good quantum number.

The present calculations concern the ground states of LiH and LiH^- with the singlet and doublet multiplicities, respectively. In constructing the wave functions, the proper permutational symmetry of the electrons has to be imposed. In the present work this is done using the spin-free formalism [18–20] that involves the construction of an appropriate symmetry projector, Y. The action of this projector on the spatial basis functions yields matrix elements that otherwise be generated by using the full (spatial plus spin) basis functions and integrating over spin coordinates. Projector Y implements the desired permutational symmetry properties. In the present work, we choose Y in the following form for LiH and LiH^-, respectively:

$$Y = (1 + P_{23})(1 + P_{45})(1 - P_{24})(1 - P_{35}) \tag{5}$$

and

$$Y = (1 + P_{23})(1 + P_{45})(1 - P_{24} - P_{26})(1 - P_{35}). \tag{6}$$

Here P_{ij} denotes the permutation of spatial coordinates of the ith and jth particles. Note that the above choice of operator Y is not unique.

In expansion (1), quantity $E_{\mathrm{rel}}^{(2)}$ corresponds to the expectation value of the Dirac–Breit Hamiltonian in the Pauli approximation, H_{rel} [21,22]. To be used in the present work, H_{rel} is first transformed from the laboratory coordinates, $\mathbf{R}_i$, to the internal coordinates, $\mathbf{r}_i$. H_{rel} includes the following terms: the mass–velocity term, H_{MV}, the Darwin term, H_{D}, the orbit–orbit interaction term, H_{OO}, and the spin–spin Fermi interaction term, H_{SS}:

$$H_{\mathrm{rel}} = H_{\mathrm{MV}} + H_{\mathrm{D}} + H_{\mathrm{OO}} + H_{\mathrm{SS}}. \tag{7}$$

The explicit forms of the corresponding effective operators in the internal coordinates are [17]:

$$H_{\mathrm{MV}} = -\frac{1}{8}\left[\frac{1}{m_0^3}\left(\sum_{i=1}^{n} \nabla_{\mathbf{r}_i}\right)^4 + \sum_{i=1}^{n} \frac{1}{m_i^3} \nabla_{\mathbf{r}_i}^4\right], \tag{8}$$

$$H_{\mathrm{D}} = -\frac{\pi}{2}\left(\sum_{i=1}^{n} \frac{q_0 q_i}{m_i^2} \delta\left(\mathbf{r}_i\right) + \sum_{\substack{i,j=1 \\ j \neq i}}^{n} \frac{q_i q_j}{m_i^2} \delta\left(\mathbf{r}_{ij}\right)\right), \tag{9}$$

$$\hat{H}_{\mathrm{OO}} = -\frac{1}{2}\sum_{i=1}^{n}\sum_{j=1}^{n}\frac{q_0 q_j}{m_0 m_j} \times \left[\frac{1}{r_j}\nabla_{\mathbf{r}_i}{}^T\nabla_{\mathbf{r}_j} + \frac{1}{r_j^3}\,\mathbf{r}_j'(\mathbf{r}_j'\cdot\nabla_{\mathbf{r}_i})\nabla_{\mathbf{r}_j}\right] + \frac{1}{2}\sum_{i=1}^{n}\sum_{j>i}^{n}\frac{q_i q_j}{m_i m_j} \times \left[\frac{1}{r_{ij}}\nabla_{\mathbf{r}_i}'\cdot\nabla_{\mathbf{r}_j} + \frac{1}{r_{ij}^3}\,\mathbf{r}_{ij}'(\mathbf{r}_{ij}^T\nabla_{\mathbf{r}_i})\nabla_{\mathbf{r}_j}\right], \tag{10}$$

and

$$H_{\mathrm{SS}} = -\frac{8\pi}{3}\sum_{\substack{i,j=1\\ j>i}}^{n}\frac{q_i q_j}{m_i m_j}\left(\mathbf{s}_i'\mathbf{s}_j\right)\delta\left(\mathbf{r}_{ij}\right). \tag{11}$$

In the last expression $\mathbf{s}_i$ denotes the spin operator of the ith pseudoparticle. The relativistic corrections are calculated as the expectation values of the above operators using the non-relativistic wave function.

3. Results

The first set of results, which is presented in Table 1, concerns the calculations of the total non-Born–Oppenheimer non-relativistic energies and leading relativistic corrections for the ground states of LiH and LiH^-. The results shown in the table are obtained with the basis sets of size that increases from 8,000 Gaussians to 14,000 Gaussians. The relativistic (or total) energies obtained by adding the relativistic corrections to the non-relativistic non-BO energies are also shown. Both energies are extrapolated to an infinite basis set size and the extrapolated values are shown in the table along with the estimated uncertainties. As one can see, both non-relativistic and relativistic energies are well converged but, as expected, the convergence is better for LiH that for LiH^-. This is mainly due to the fact that the former system contains one electron less than the latter. It is usually the case that for a system with fewer particles one needs a smaller number of the basis functions to converge the calculations to the same accuracy level as for a system with more particles.

The results shown in Table 1 are obtained in the basis set growing process that involves starting from a small set of Gaussians with nonlinear parameters chosen by a combination of a random and physically-motivated choices. After that the growing process involves a set of steps, where in each step the basis set is enlarged by addition of a subset of new Gaussians and variationally optimising them with the a procedure that employs the analytical energy gradient. The enlargement and subsequent optimisation are done using a one-function-at-a-time approach. The initial guess of a new function is generated stochastically based on the values of nonlinear parameters of the Gaussian already included in the basis set. Several hundred of such stochastically generated candidates are tried and the best one is retained. Then the newly added function is variationally optimised and, if it is not linearly dependent with all other functions in the set, it is included in the basis set. The L_k matrix elements and the m_k power in the r_1 preexponential factor are subject to the optimisation. As mentioned, the m_k powers are optimised in the 0–200 range and are restricted to be even integers. After a certain number of Gaussians are added, the nonlinear parameters of all function in the basis set generated so far are reoptimised, again using a one-function-at-a-time approach. In this reoptimisation, however, only the L_k matrix elements are varied, while the m_k values kept unchanged.

We find it interesting to compare the distributions of powers, m_k, that result from the optimisations of the basis sets performed for the ground-state wave functions of LiH and LiH^-. They are shown in Figure 1. Upon examining the histograms, one can make the following observations. The power distributions are very similar for both systems. The most frequently occuring powers have values in the range from 10 to 50. After that, the probability of the appearance of a certain value of the power decreases with the increasing value of the power. However, even as the powers approach the limiting value of 200, there is a non-zero probability of finding such powers in the basis sets of the two systems. One can notice a small maximum of the distribution of the powers near 200. This maximum indicates that, if the power range were extended, the variational optimisation might have yielded a few functions with powers larger than 200. However, the range of 0–200 we used in our calculations of the ground states of LiH and LiH^- is fairly adequate.

In the next step the non-relativistic and relativistic energies of LiH and LiH^- given in Table 1 are used to calculate the the electron affinity of LiH. The results are shown in Table 2. The energy of LiH^- converges slower with the number of ECGs than the LiH energy. Since the LiH^- energy lies lower than the energy of LiH, the electron affinity calculated as the difference of the LiH^- and LiH energies effectively provides an lower bound to the exact electron affinity value. The EAs calculated in the present work are compared in Table 2 with the experimental value and with some theoretical calculations reported in the literature. As one can see, the EA results obtained at both the non-relativistic and relativistic levels of the theory agree with the experimental result of Sarkas *et al.* [9] to within the experimental uncertainty. Among the previously calculated EAs of LiH, the MRCISD+Q

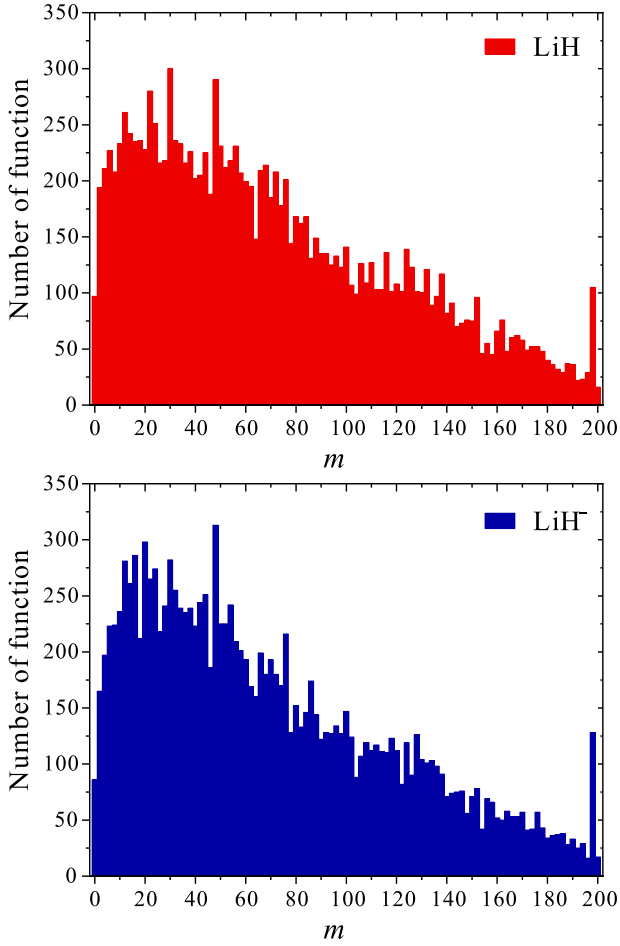

Figure 1. A comparison of the the distributions of the m_k powers of r_1-prefactors in the Gaussians obtained in the optimisation of the basis sets for LiH and LiH$^-$.

Table 2. Convergence of the electron affinities (EA) of LiH (in eV) in terms of the number of the basis functions.

Basis(LiH)	Basis (LiH$^-$)	EA_{nr}	EA_{rel}
8,000	8,000	0.332648	0.332609
10,000	10,000	0.332818	0.332776
12,000	12,000	0.332919	0.332879
14,000	14,000	0.332990	0.332951
∞	∞	0.333012(11)	0.332979(31)
CCSDT [13]		0.327	
MRCISD+Q [14]		0.332	
FN-DMC [23]		0.340(4)	
CCSD(T) [24]		0.334 ± 0.001	
Exp. [9]		0.342 ± 0.012	

Note: The numbers in the first two columns show the number of ECG functions employed in the calculations.

value [14] best agrees with our non-relativistic result of 0.332990 a.u. (extrapolated to 0.333012(11) a.u.).

The non-Born–Oppenheimer non-relativistic wave functions obtained for LiH and LiH$^-$ with the largest basis set generated for the two systems in this work are used to calculate some expectation values of interparticle distances and their squares, as well as the most probable Li-H internuclear distance. The expectation values of the interparticle Dirac delta functions are also calculated. The results are shown in Table 3. The attachment of an excess electron in LiH increases the average internuclear distance from 3.0610383(13) to 3.214425(10) a.u. Also, the average proton–electron distance increases from 2.5651045(9) to 4.03936(20) a.u. This increase can be explained as follows. The neutral LiH molecule is an ionic $\mathrm{Li}(+\delta) - H(-\delta)$ species in the ground state due to a higher electron affinity of the hydrogen atom than the lithium atom. Thus, in the formation of LiH$^-$, the excess electron mostly localises near the lithium atom resulting in an increase of the average proton-electron distance. Also, as the neutral LiH has a rather large dipole moment (5.882 ± 0.003; Wharton *et al.* [25]), a significant part of the electron attachment to LiH is due to the dipole-electron interaction that results in the excess electron occupying a dipole-bound state that extends away from the lithium atom outside the molecule. This results in an additional increase of the proton–electron distance, as well as the distance between the lithium nucleus and the electron. Also, the electron attachment makes the electron density in the molecule to become more diffused resulting in the $\langle\delta(\mathbf{r}_{\mathrm{H}-e})\rangle$ expectation value to decrease from 0.095073(15) to 0.074684(11) a.u. (see Table 3).

Table 3. Expectation values of the interparticle distances, $\langle r_{ij}\rangle$, and the most probable distance between Li and H nuclei, $r^{\mathrm{mp}}_{\mathrm{Li-H}}$, calculated with the LiH and LiH$^-$ non-Born–Oppenheimer wave functions obtained with the largest basis sets generated in this work.

		LiH	LiH$^-$
$\langle r_{\mathrm{Li-H}}\rangle$		3.0610383(13)	3.214425(10)
$\langle r_{\mathrm{Li-e}}\rangle$		1.9719334(5)	3.13005(22)
$\langle r_{\mathrm{H-e}}\rangle$		2.5651045(9)	4.03936(20)
$\langle r_{\mathrm{e-e}}\rangle$		2.9559396(8)	5.27574(41)
$r^{\mathrm{mp}}_{\mathrm{Li-H}}$		3.013130(5)	3.157615(3)
$r^{\mathrm{mp}}_{\mathrm{Li-H}}$	BO ECG[a]	3.04482(5)	
$r^{\mathrm{mp}}_{\mathrm{Li-H}}$	CCSD(T)[b]	3.0275(4)	3.1740(4)
r_0	MRCISD+Q [14][c]	3.019015695	3.184011222
$\langle r^2_{\mathrm{Li-H}}\rangle$		9.419705(8)	10.39224(5)
$\langle r^2_{\mathrm{Li-e}}\rangle$		6.585742(4)	20.062(7)
$\langle r^2_{\mathrm{H-e}}\rangle$		7.745214(7)	28.419(7)
$\langle r^2_{\mathrm{e-e}}\rangle$		10.966067(7)	43.792(14)
$\langle\delta(\mathbf{r}_e)\rangle$		3.451766(17)	2.7579(8)
$\langle\delta(\mathbf{r}_{\mathrm{H}-e})\rangle$		0.095073(15)	0.074684(11)
$\langle\delta(\mathbf{r}_{e-e})\rangle$		0.091647(30)	0.054860(8)

Notes: The results are compared with the values obtained in the Born–Oppenheimer ECG [26] and MRCISD+Q [14] calculations. All values are expressed in atomic units.[a]Born–Oppenheimer calculations with 2,400 ECG basis functions [26].[b]Coupled-cluster singles and doubles and non-iterative triple excitations. The aug-cc-pV5Z [27] basis set has been used. The calculations were carried out using the Gaussian 16 software package [28].[c]The internally contracted configuration interaction in the single and double space (MRCISD) level with four electrons distributed among the five orbitals (MRCISD+Q) arising from the 1*s*, 2*s*, and 2*p* atomic orbitals in the multiconfigurational self-consistent-field (MCSCF) part of the calculations has been used.

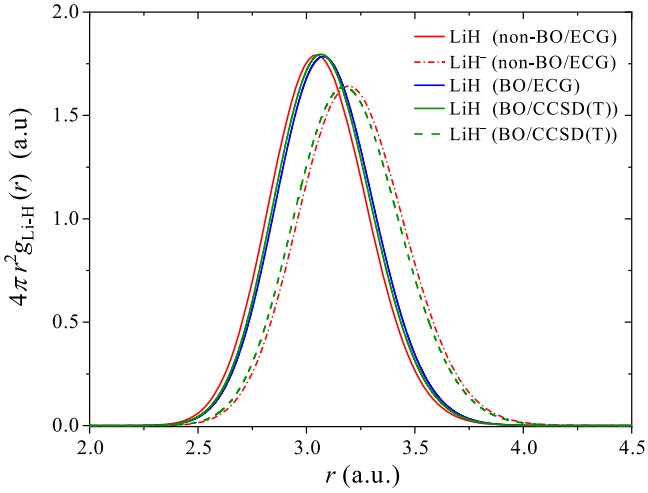

Figure 2. The nucleus–nucleus pair correlation functions for the ground states of LiH and LiH^- molecules calculated at different levels of theory.

Lastly, in Figure 2, the nucleus–nucleus pair correlation functions calculated for the ground states of LiH and LiH^- using the respective non-Born–Oppenheimer wave functions in the largest basis sets of 14,000 ECGs generated in this work are compared with the square of the corresponding vibrational wave functions obtained using different approaches based on the Born–Oppenheimer approximation. As one can see, the density of the proton for the two systems is localised around the respective average distance and it is slightly less sharply peaked and broader for LiH^- than for LiH. The pictures obtained from both the present non-BO approach and from the BO calculations are very similar both in terms of the heights, the broadness, and the relative shift of the LiH and LiH^- peaks.

4. Summary

In this work we present the most accurate non-Born–Oppenheimer calculations ever performed for a molecule with five electrons. As a result of several months of continuous optimisations, basis sets containing 14,000 explicitly correlated all-particle Gaussian basis functions are generated for the LiH and LiH^- molecules. Then the leading relativistic energy corrections are calculated and added to the non-BO non-relativistic energies. These are used to calculated the LiH electron affinity. The obtained value is likely the most accurate EA result ever calculate.

Disclosure statement

No potential conflict of interest was reported by the author(s).

Funding

This work has been supported by Nazarbayev University [faculty development grant No. 021220FD3651], and the National Science Foundation [grant number 1856702]. L.A. acknowledges the support of the Centre for Advanced Study (CAS), the Norwegian Academy of Science and Letters, in Oslo, Norway, which funds and hosts our research project titled: Attosecond Quantum Dynamics Beyond the Born–Oppenheimer Approximation, during the 2021–2022 academic year. The authors are grateful to the University of Arizona Research Computing for providing computational resources for this work. Part of the calculations were performed on Shabyt HPC cluster at Nazarbayev University.

References

[1] W. Kołos and L. Wolniewicz, Rev. Mod. Phys. **35** (3), 473–483 (1963). doi:10.1103/RevModPhys.35.473.
[2] W. Kołos and L. Wolniewicz, J. Chem. Phys. **41** (12), 3663–3673 (1964). doi:10.1063/1.1725796.
[3] W. Kołos and L. Wolniewicz, J. Chem. Phys. **43** (7), 2429 (1965). doi:10.1063/1.1697142.
[4] D.B. Kinghorn and R.D. Poshusta, Phys. Rev. A **47** (5), 3671–3681 (1993). doi:10.1103/PhysRevA.47.3671.
[5] S. Bubin and L. Adamowicz, J. Chem. Phys. **121** (13), 6249–6253 (2004). doi:10.1063/1.1786580.
[6] J. Carlsten, J. Peterson, and W. Lineberger, Chem. Phys. Lett. **37** (1), 5–8 (1976). doi:10.1016/0009-2614(76)80148-0.
[7] S.E. Novick, P.L. Jones, T.J. Mulloney, and W. Lineberger, J. Chem. Phys. **70** (5), 2210–2214 (1979). doi:10.1063/1.437777.
[8] T.M. Miller, D.G. Leopold, K.K. Murray, and W. Lineberger, J. Chem. Phys. **85** (5), 2368–2375 (1986). doi:10.1063/1.451091.
[9] H.W. Sarkas, J.H. Hendricks, S.T. Arnold, and K.H. Bowen, J. Chem. Phys. **100** (3), 1884–1888 (1994). doi:10.1063/1.466540.
[10] K. Jordan, K. Griffing, J. Kenney, E. Andersen, and J. Simons, J. Chem. Phys. **64** (11), 4730–4740 (1976). doi:10.1063/1.432059.
[11] B.K. Lee, J.M. Stout, and C.E. Dykstra, J. Mol. Struct.: THEOCHEM **400**, 57–68 (1997). doi:10.1016/S0166-1280(97)00082-1.
[12] S.B. Sharp and G.I. Gellene, J. Chem. Phys. **113** (15), 6122–6131 (2000). doi:10.1063/1.1308545.
[13] G.L. Gutsev, M. Nooijen, and R.J. Bartlett, Phys. Rev. A **57**, 1646–1651 (1998). doi:10.1103/PhysRevA.57.1646.
[14] D.T. Chang, K. Reimann, G. Surratt, G.I. Gellene, P. Lin, and R.R. Lucchese, J. Chem. Phys. **117** (12), 5757–5763 (2002). doi:10.1063/1.1502246.
[15] W.E. Caswell and G.P. Lepage, Phys. Lett. B **167** (4), 437–442 (1986). doi:10.1016/0370-2693(86)91297-9.
[16] K. Pachucki, Phys. Rev. A **56**, 297–304 (1997). doi:10.1103/PhysRevA.56.297.
[17] S. Bubin, M. Pavanello, W.C. Tung, K.L. Sharkey, and L. Adamowicz, Chem. Rev. **113** (0), 36–79 (2013). doi:10.1021/cr200419d.
[18] F.A. Matsen and R. Pauncz, *The Unitary Group in Quantum Chemistry* (Elsevier, Amsterdam, 1986).
[19] R. Pauncz, *Spin Eigenfunctions* (Plenum, New York, 1979).

[20] M. Hamermesh, *Group Theory and Its Application to Physical Problems* (Addison-Wesley, Reading, MA, 1962).
[21] H.A. Bethe and E.E. Salpeter, *Quantum Mechanics of One- and Two-Electron Atoms* (Plenum, New York, 1977).
[22] A.I. Akhiezer and V.B. Berestetskii, *Quantum Electrodynamics* (John Wiley & Sons, New York, 1965).
[23] G. Morosi, M. Mella, and D. Bressanini, J. Chem. Phys. **111** (15), 6755–6758 (1999). doi:10.1063/1.479972.
[24] D. Feller, J. Chem. Phys. **144** (1), 014105 (2016). doi:10.1063/1.4939184.
[25] L. Wharton, L.P. Gold, and W. Klemperer, J. Chem. Phys. **33** (4), 1255–1255 (1960). doi:10.1063/1.1731368.
[26] W.C. Tung, M. Pavanello, and L. Adamowicz, J. Chem. Phys. **134** (6), 064117 (2011). doi:10.1063/1.3554211.
[27] B.P. Pritchard, D. Altarawy, B. Didier, T.D. Gibson, and T.L. Windus, J. Chem. Inf. Model. **59** (11), 4814–4820 (2019). doi:10.1021/acs.jcim.9b00725.
[28] M.J. Frisch, G.W. Trucks, H.B. Schlegel, G.E. Scuseria, M.A. Robb, J.R. Cheeseman, G. Scalmani, V. Barone, G.A. Petersson, H. Nakatsuji, X. Li, M. Caricato, A.V. Marenich, J. Bloino, B.G. Janesko, R. Gomperts, B. Mennucci, H.P. Hratchian, J.V. Ortiz, A.F. Izmaylov, J.L. Sonnenberg, D. Williams-Young, F. Ding, F. Lipparini, F. Egidi, J. Goings, B. Peng, A. Petrone, T. Henderson, D. Ranasinghe, V.G. Zakrzewski, J. Gao, N. Rega, G. Zheng, W. Liang, M. Hada, M. Ehara, K. Toyota, R. Fukuda, J. Hasegawa, M. Ishida, T. Nakajima, Y. Honda, O. Kitao, H. Nakai, T. Vreven, K. Throssell, J.A. Montgomery, Jr., J.E. Peralta, F. Ogliaro, M.J. Bearpark, J.J. Heyd, E.N. Brothers, K.N. Kudin, V.N. Staroverov, T.A. Keith, R. Kobayashi, J. Normand, K. Raghavachari, A.P. Rendell, J.C. Burant, S.S. Iyengar, J. Tomasi, M. Cossi, J.M. Millam, M. Klene, C. Adamo, R. Cammi, J.W. Ochterski, R.L. Martin, K. Morokuma, O. Farkas, J.B. Foresman, and D.J. Fox, Gaussian 16 Revision C.01. Gaussian Inc., Wallingford CT, 2016.